

Title	Experimental observations of instabilities in rotating plane Couette flow
Author(s)	Hiwatashi, K; Alfredsson, PH; Tillmark, N; Nagata, M
Citation	PHYSICS OF FLUIDS (2007), 19(4)
Issue Date	2007-04
URL	<a href="http://hdl.handle.net/2433/50206">http://hdl.handle.net/2433/50206</a>
Right	Copyright 2007 American Institute of Physics. This article may be downloaded for personal use only. Any other use requires prior permission of the author and the American Institute of Physics.
Type	Journal Article
Textversion	publisher; none

## Experimental observations of instabilities in rotating plane Couette flow

Kazuaki Hiwatashi<sup>a)</sup>

Department of Aeronautics and Astronautics, Kyoto University, Kyoto 606-8501, Japan

P. H. Alfredsson<sup>b)</sup> and Nils Tillmark

Linné Flow Centre, KTH Mechanics, Royal Institute of Technology, S-100 44 Stockholm, Sweden

M. Nagata

Department of Aeronautics and Astronautics, Kyoto University, Kyoto 606-8501, Japan

(Received 16 December 2006; accepted 15 February 2007; published online 17 April 2007)

The transition from the two-dimensional (2D) longitudinal roll cell state to 3D flows in the rotating plane Couette system, predicted by the theoretical investigation [M. Nagata, *J. Fluid Mech.* **358**, 357 (1998)], is examined experimentally. The streamwise and spanwise wave numbers of observed *steady* 3D flows seem to agree with those predicted by the theory when the rotation rate is relatively large. However, we observe *unsteady* 3D states in the region where the theory predicts stable steady 3D flows when the rotation rate is small. © 2007 American Institute of Physics.

[DOI: 10.1063/1.2716767]

Nagata<sup>1</sup> analyzed the bifurcation of a three-dimensional (3D) tertiary flow from the 2D roll cell state in rotating plane Couette system theoretically. In a follow-up paper, Nagata<sup>2</sup> showed that the tertiary flow could be stable for some parameter range. So far, rigorous experimental investigations on such flows have not been done. In the present Brief Communication, we examine the transition to tertiary flows experimentally.

The physical configuration of our rotating plane Couette system is shown schematically in Fig. 1.

The plane Couette channel constructed by Tillmark and Alfredsson<sup>3</sup> is placed here on a turntable. The Couette flow is established by an endless transparent polyester plastic belt, which is guided by four small and two large (diameter 70 and 200 mm, respectively) cylinders. The Couette channel flow is established where the band moves along two glass walls, one that is one wall of the large water compartment (overall length 2.5 m, height 0.4 m) and one that is a movable wall inside the compartment. The width of the channel can be changed by the positioning of the inner wall. By adjusting the small guiding cylinders, a thin lubricating water film is established between the band and the glass walls. In the present experiments, the gap,  $2h$ , between the two sides of the channel is nominally 10 mm. The actual distance is measured optically by a microscope. The belt is driven by one of the large cylinders with a tacho controlled dc motor and the belt speed is monitored through another tacho-generator mounted on the other large cylinder, which is driven by the belt itself.

The turntable is driven by a dc motor with a tacho-generator in a feedback system. The maximum angular velocity of the turntable is  $\Omega_0 = 0.53$  rad/s with variation of about 1%. The working fluid is water and is seeded with

light-reflecting platelets (Merck, Iriodin 120) for flow visualization.

Visualized flow fields are recorded by a video camera (Panasonic DMC-FX9). The video recording has a time resolution of 10 frames per second and a capability of recording for 20 min with a 512 Mbyte memory card. The wavelength is measured directly from the photographic frames.

The water temperature  $T$  varied between 17.7 and 19.5°C during the period (2 weeks) of the experiments. The values of the kinematic viscosity  $\nu$  are  $1.139 \times 10^{-6}$  m<sup>2</sup>/s at 15°C and  $1.0038 \times 10^{-6}$  m<sup>2</sup>/s at 20°C. Using these values for a linear interpolation, we approximate  $\nu(T)$  by

$$\nu(T) = (1.5446 - 0.02704 \times T) \times 10^{-6} \text{ m}^2/\text{s} \quad (1)$$

The motion of the rotating plane Couette flow is governed by two nondimensional parameters: the Reynolds number  $R$  and the rotation number  $\Omega$ . They are defined by

$$R = \frac{Vh}{\nu}, \quad \Omega = \frac{2\Omega_0 h^2}{\nu}, \quad (2)$$

respectively, where  $V$  is the translational velocity of the belt.

First, we examine the stability of the laminar flow. It is well known that the critical Reynolds number for the onset of roll cell instabilities in the rotating plane Couette flow is given by

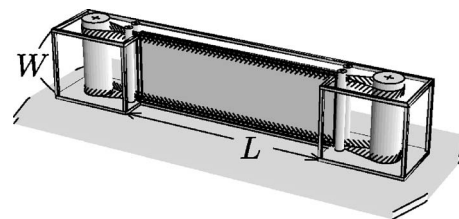


FIG. 1. The schematic diagram of the rotating plane Couette flow apparatus.  $L = 1500$  mm,  $W = 400$  mm.

<sup>a)</sup>Electronic mail: kazuaki\_hiwatashi@kuaero.kyoto-u.ac.jp

<sup>b)</sup>Electronic mail: hal@mech.kth.se

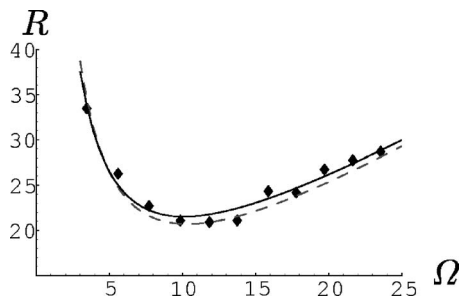


FIG. 2. The neutral curve for the roll cell instability. Black diamond  $\blacklozenge$  indicates experimental results and the dashed curve is given by (3). The solid curve corresponds to (4).

$$R = \Omega + 107/\Omega. \quad (3)$$

To determine the critical Reynolds number experimentally, we increase the belt speed gradually while keeping the rotation rate constant. In Fig. 2, we plot black diamonds indicating the points where the roll cell instability sets in. The solid curve in the figure is drawn by applying the least-squares method to the data points to fit the expression

$$R = a\Omega + b + c/\Omega, \quad (4)$$

for the unknown constants  $a$ ,  $b$ , and  $c$ . The obtained values of  $a$ ,  $b$ , and  $c$  are  $a=0.952$ ,  $b=2.28$ , and  $c=97.2$ .

The roll cell state instability contains a 2D structure that is periodic in the rotational axis. As the Reynolds number is increased above the black dots, the 2D roll cell state attains a finite amplitude. We find that the wavelength of the roll cell at the upper part inside the glass panels is shorter than that at the lower part, as shown in Fig. 3. The values of wavelength are 1.8 cm at the upper part, 2.0 cm in the middle, and 2.6 cm at the lower part, corresponding to the wave numbers, 1.7, 1.6, and 1.2, respectively. The wave number in the middle corresponds better to the theoretical value 1.559. The difference in wave numbers seems to result from the different boundary conditions at the top and the bottom (free surface at the top and rigid end at the bottom).

By increasing the Reynolds number further, transition to 3D flows occurs. In this Brief Communication, experimental observations are particularly concentrated on three cases:  $(R, \Omega) = (48.4, 5.51)$ ,  $(101, 1.73)$ , and  $(100, 9.31)$ . We note that the theory predicts stable tertiary flows for  $4.75 < \Omega$

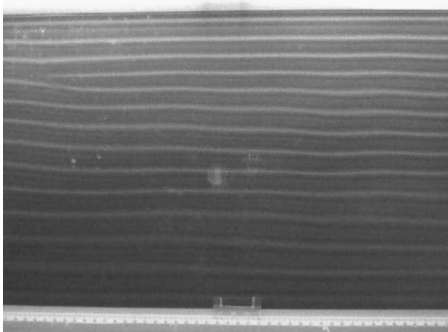


FIG. 3. The 2D roll cells. We note that the intervals between the cells at the lower part are longer than those at the upper part.  $R=49.9$  and  $\Omega=9.49$ .



FIG. 4. The 3D flow obtained experimentally.  $R=100, \Omega=9.31$ .

$< 6.63$  when  $R=50$  and for  $1.63 < \Omega < 1.85$  and  $8.0 < \Omega < 10.5$  when  $R=100$  (see Nagata<sup>2</sup>), so that we would expect to observe steady 3D flows in all of the three cases.

We observe a stable 3D structure at  $R=100, \Omega=9.31$  as shown in Fig. 4. The observed streamwise wave numbers vary between 0.4 and 0.35 and the wavelength in the rotational direction is almost unchanged from that of the 2D roll cell state. The typical streamwise wave number used for finding a stable tertiary solution by Nagata<sup>2</sup> is equal to 0.5 for  $R=100$  and  $8.0 < \Omega < 10.5$ . Therefore, we conclude that the flow pattern observed for this case corresponds to the stable steady solution reported by Nagata.<sup>2</sup> We add that the spanwise wavelength of the observed 3D flow has a similar tendency to that of the roll cell flow, that is, it is longer at the lower part than at the upper part of the channel.

We also observe a transition to a 3D flow for the case  $R=48.4, \Omega=5.51$ , although the 3D structure of the flow field is less clear than the previous case.

For both cases, an oscillation of flow pattern with a steady period is observed. The period of the flow pattern oscillation and the period of the table rotation for both cases and some additional cases are compared in Table I. Comparison of the periods leads us to conclude that the oscillation of the flow pattern is driven by noises from the table rotation and is not an intrinsic feature of the flow patterns.

TABLE I. The oscillation periods.

$R$	$\Omega$	Period of oscillation (s)	Period of rotating table (s)
48.4	5.51	54.0	54.2
100	5.61	53.0	53.1
51	5.61	53.5	53.5
100	9.31	31.8	32.0
149	9.31	32.2	32.0

TABLE II. The states of flow field observed at every 10 s. A, Pure Couette flow; B, roll cell state; C, 3D flow state. It requires a comparatively long time to complete a transition to the 3D state at  $R=48.4$  and  $\Omega=5.51$ .

$R$	$\Omega$	10 s	20	30	40	50	180
48.4	5.51	A	A	B	B	B	C
100	5.61	A	B	B	B	C	C
100	9.31	A	B	B	C	C	C
151	5.61	A	B	C	C	C	C
149	9.31	A	B	C	C	C	C

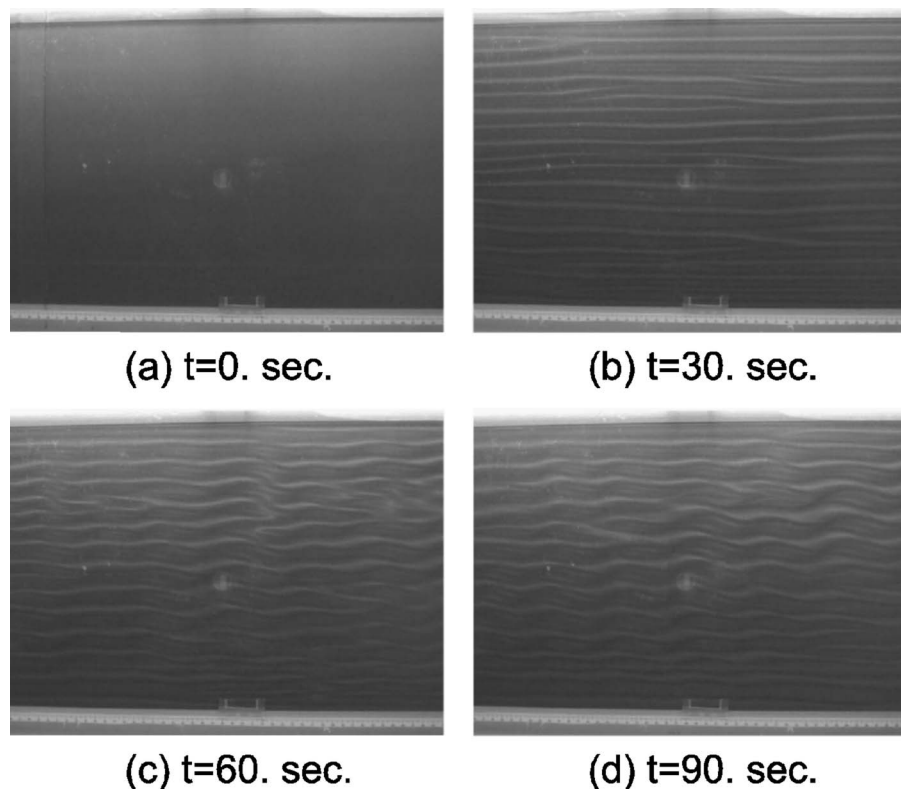


FIG. 5. Sequential changes of the flow field at every 30 s from started recording.  $R=100, \Omega=9.31$ .

3D structures of flow pattern are observed at all the parameter values in Table I. As  $R$  is increased, the flow pattern becomes sensitive and breaks down, yet still keeping its three dimensionality. After the pattern breaks down, it returns to its original 3D state in a few minutes.

The flow field observed at every 10 s from the start of recording is shown in Table II. The sequential photos in Fig. 5 are taken at every 30 s from the start of recording at  $R=100$  and  $\Omega=9.31$ . In every case in Table II the pure Couette flow state changes to a 2D roll cell state followed by a 3D flow.

In contrast to the two cases described above, steady 3D

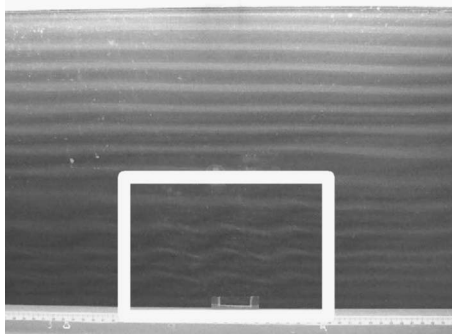


FIG. 6. The flow field at  $R=101, \Omega=1.73$ . A 3D structural pattern can be seen inside the boxed region. This pattern appears and vanishes repeatedly with a period of a few minutes.

patterns are *not* observed at  $R=101$  and  $\Omega=1.73$ . Although the transition from the 2D roll cell state to a 3D flow does occur temporarily (see Fig. 6), the 3D flow pattern does not keep its structure for a long time and it returns to the 2D roll cell state. This sequence occurs repeatedly. The region where this temporal transition occurs is restricted to the lower part of the observation area. The alternating appearance of the 3D and 2D flow structures seems to be explained by the recent theoretical findings by Nagata and Kawahara<sup>4</sup> where 3D periodic solutions as a quaternary flow at  $R=100$  collide with a secondary solution (2D roll cell state) to form a homoclinic connection as the rotation rate is varied.

In conclusion, we have reported that for certain parameter ranges in rotating plane Couette flow, a transition from 2D roll cells to steady 3D flow states has been observed experimentally. Such a transition has previously only been obtained theoretically. For another parameter range where theory also predicts a steady 3D state, the experiments show an unsteady state.

<sup>1</sup>M. Nagata, "Bifurcations in Couette flow between almost corotating cylinders," *J. Fluid Mech.* **169**, 229 (1986).

<sup>2</sup>M. Nagata, "Tertiary solutions and their stability in rotating plane Couette flow," *J. Fluid Mech.* **358**, 357 (1998).

<sup>3</sup>N. Tillmark and P. H. Alfredsson, "Experiments on transition in plane Couette flow," *J. Fluid Mech.* **235**, 89 (1992).

<sup>4</sup>M. Nagata and G. Kawahara, "Three-dimensional periodic solutions in rotating/non-rotating plane Couette flow," in *Advances in Turbulence X* (CIMNE, Barcelona, 2004), p. 557.